Electronic Supplementary Information

Sonochemically induced cube-shaped $NiFe_2O_4$ nanoparticles catalyzed selective oxidation of benzyl alcohol to benzaldehyde

Saddam Iraqui, Babul Kalita, and Md. Harunar Rashid*

Department of Chemistry, Rajiv Gandhi University, Rono Hills, Doimukh 791 112, Arunachal Pradesh, India

Corresponding author email: harunar.rashid@rgu.ac.in

Contents

1. Leaching study
2. Characterization techniques
3. TEM image (Figure S1)
4. XPS survey scan of before and after catalysis (Figure S2)
5. Characterization of the catalyzed products
6. NMR spectra of the products (Figure S3-S18)
7. Reference

Leaching study

For the leaching study, the reaction mixture was filtered after the completion of the catalyzed reaction. The filtrate was then evaporated in a heating mantle and the residue was dissolved in a solution of HNO_3 (1 mL HNO_3 in 4 mL water) for quantitative analysis of Fe in an atomic absorption spectrometer (AAS).

Characterization of the product

X-ray diffraction (XRD) study of the dried powder samples was carried out on a Phillips X'Pert Pro Powder X-ray diffractometer using Cu *k*α radiation with a wavelength of 0.154 nm at an accelerating voltage of 40 kV with 35 mA current. For transmission electron microscopic (TEM) studies, a drop of an aqueous suspension of an individual powder sample was cast on a carbon-coated copper grid. The excess solutions were soaked with tissue paper followed by drying in the air. The micrographs were then recorded in a high–resolution JEOL electron microscope (JEM 2100EM) at an accelerating voltage of 200 kV. The dried powder of the samples was subjected to magnetic measurements at room temperature using a Quantum Design 7T SQUID magnetometer. X-ray photoelectron spectroscopy (XPS) analyses of the dried powder samples were performed in SPECS Germany made ESCA spectrometer. ^{57}Fe Mössbauer spectroscopy study was performed in transmission mode using a PC-based Mossbauer spectrometer having 1024 channels MCA card operating in the constant acceleration mode. All measurements were carried out in transmission geometry using a 20 mCi, ^{57}Co source in Rh matrix. The spectrometer was calibrated with a 12 μm thick high-purity natural iron foil. The N_2 gas adsorption-desorption isotherms of the products were recorded at 77 K (Quantachrome Nova 1000 Instrument) after degassing the powder samples at 150 ºC for 4.0 h in an inert atmosphere. The melting points of the purified samples were measured using a Buchi melting point M-560 instrument. ^{1}H and ^{13}C NMR spectra were recorded in a JNM

ECS 400 MHz NMR spectrophotometer (JEOL) and an Advance NEO 500 MHz NMR spectrophotometer (Bruker) using tetramethylsilane (TMS) as the internal standard. Chemical shift values and coupling constants are expressed in ppm and Hertz (Hz) respectively.

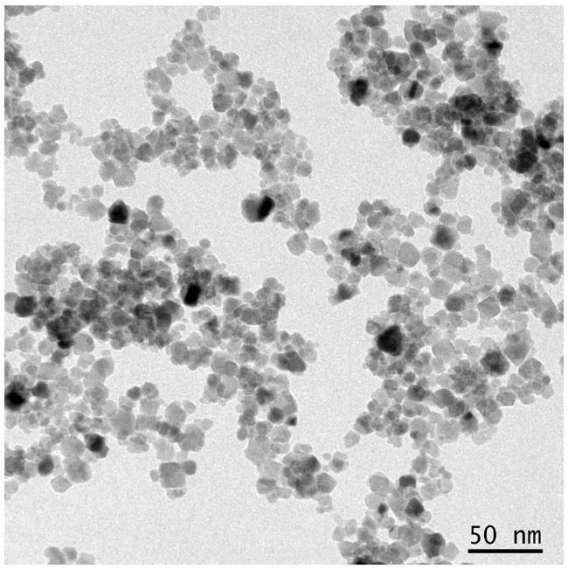

Figure S1. TEM images of $NiFe_2O_4$ NPs prepared in the absence of any additive.

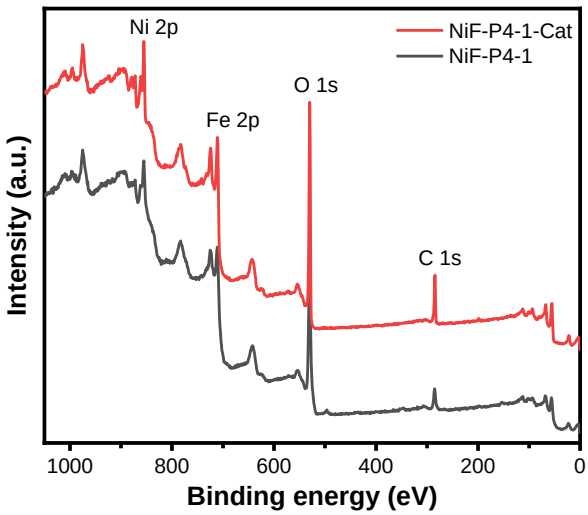

Figure S2. XPS survey scan spectrum of $NiFe_2O_4$ NPs before (NiF-P4-1) and after catalysis (NiF-P4-1-Cat).

Characterization of the catalytic products

Entry 1; Table 5: Benzaldehyde

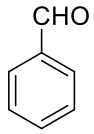

Physical appearance: Colourless liquid

^{1}H NMR ($CDCl_3$, 400 MHz): δ 9.87 (*s*, 1H), 7.74 (*d*, *J*=8 Hz, 2H), 7.48 (*t*, *J*=8 Hz, 2H), 7.38 (*t*, *J*=8 Hz, 1H) ppm

^{13}C NMR ($CDCl_3$, 100 MHz): 192.45, 136.37, 134.47, 129.72, 128.99 ppm

Entry 2; Table 5: 2-nitrobenzaldehyde

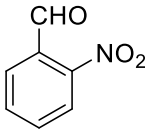

Physical appearance: White solid; melting point (mp) = 43-46 °C

^{1}H NMR ($CDCl_3$, 500 MHz): δ 10.40 (*s*, 1H), 8.09 (*t*, *J*=4.5 Hz, 1H), 7.94-7.93 (*m*, 1H), 7.80-7.73 (*m*, 2H) ppm

^{13}C NMR ($CDCl_3$, 125 MHz): δ 188.13, 149.93, 134.06, 133.68, 131.23, 129.59, 124.46 ppm

Entry 4; Table 5: 2-chlorobenzaldehyde

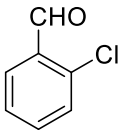

Physical appearance: Yellow coloured liquid

^{1}H NMR ($CDCl_3$, 400 MHz): δ 10.48 (*s*, 1H), 7.93-7.91 (*m*, 1H), 7.55-7.50 (*m*, 1H), 7.48-7.40 (*m*, 1H), 7.37 (*d*, *J*=8 Hz, 1H) ppm

^{13}C NMR ($CDCl_3$, 100 MHz): 189.91, 135.16, 133.39, 132.34, 131.44, 130.65, 126.71 ppm

Entry 5; Table 5: 4-nitrobenzaldehyde

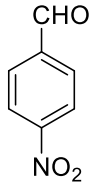

Physical appearance: Pale yellow solid; melting point (mp) = 104-106 °C

^{1}H NMR ($CDCl_3$, 400 MHz): δ 10.17 (*s*, 1H), 8.41 (*d*, *J*=8.8 Hz, 2H), 8.08 (*d*, *J*=8.8 Hz, 2H) ppm

^{13}C NMR ($CDCl_3$, 125 MHz): δ 190.38, 151.22, 140.12, 130.57, 124.40 ppm

Entry 6; Table 5: 4-bromobenzaldehyde

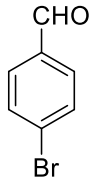

Physical appearance: White solid; melting point (mp) = 55-57 °C

^{1}H NMR ($CDCl_3$, 400 MHz): δ 9.97 (*s*, 1H), 7.74 (*d*, *J*=8 Hz, 2H), 7.68 (*d*, *J*=8 Hz, 2H) ppm

^{13}C NMR ($CDCl_3$, 100 MHz): 191.26, 135.20, 132.67, 131.12, 129.86 ppm

Entry 7; Table 5: 4-chlorobenzaldehyde

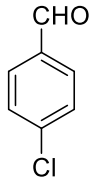

Physical appearance: Pale yellow powder; melting point (mp) = 45-47 °C

^{1}H NMR ($CDCl_3$, 400 MHz): δ 9.93 (*s*, 1H), 7.77 (*d*, *J*=8 Hz, 2H), 7.46 (*d*, *J*=8 Hz, 2H) ppm

^{13}C NMR ($CDCl_3$, 100 MHz): 190.97, 141.02, 134.85, 131.03, 129.54 ppm

Entry 10; Table 5: 4-methoxybenzaldehyde

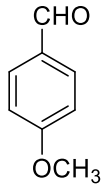

Physical appearance: Light yellow liquid

^{1}H NMR ($CDCl_3$, 500 MHz): δ 9.87 (*s*, 1H), 7.83 (*t*, *J*=4.25 Hz, 2H), 6.99 (*t*, *J*=4.25 Hz, 2H), 3.88 (*s*, 3H) ppm

^{13}C NMR ($CDCl_3$, 125 MHz): δ 191.10, 164.86, 132.51, 130.12, 114.59, 55.83 ppm

Benzoic acid[1]

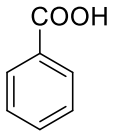

Physical appearance: white crystals; melting point (mp) = 121-122 °C

^{1}H NMR ($CDCl_3$, 400 MHz): δ 8.13 (*d*, *J*= 8 Hz, 2H), 7.62 (*t*, *J*= 8 Hz), 7.49 (*t*, *J*= 8 Hz, 2H) ppm

^{13}C NMR ($CDCl_3$, 100 MHz): δ 171.90, 133.81, 130.23, 129.32, 128.52 ppm

^{1}H and ^{13}C NMR spectra of selected isolated products

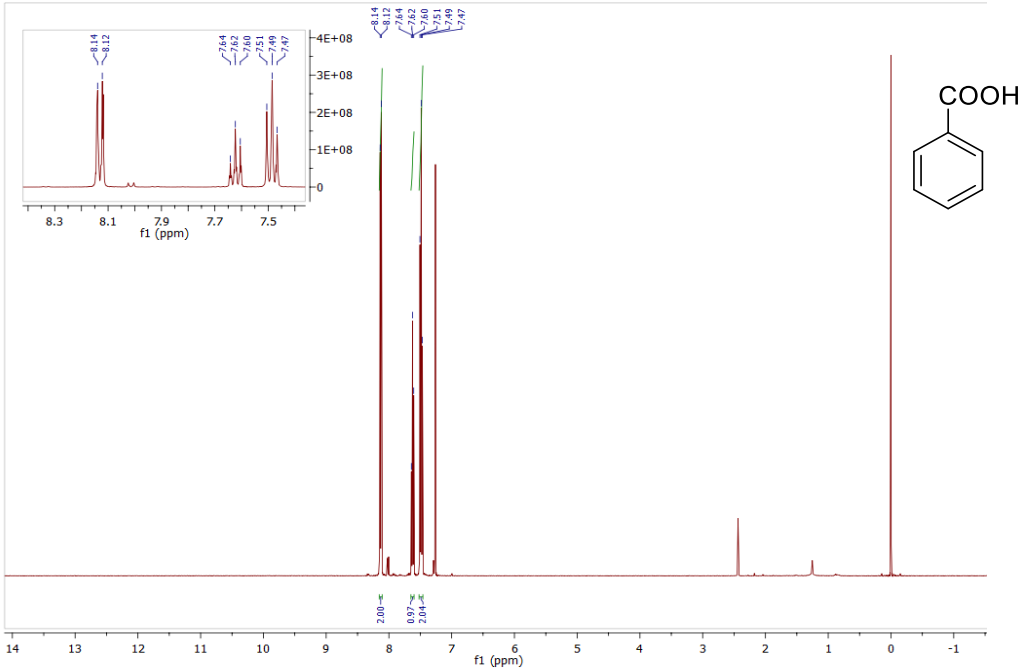

Figure S3. ^{1}H NMR spectrum of benzoic acid.

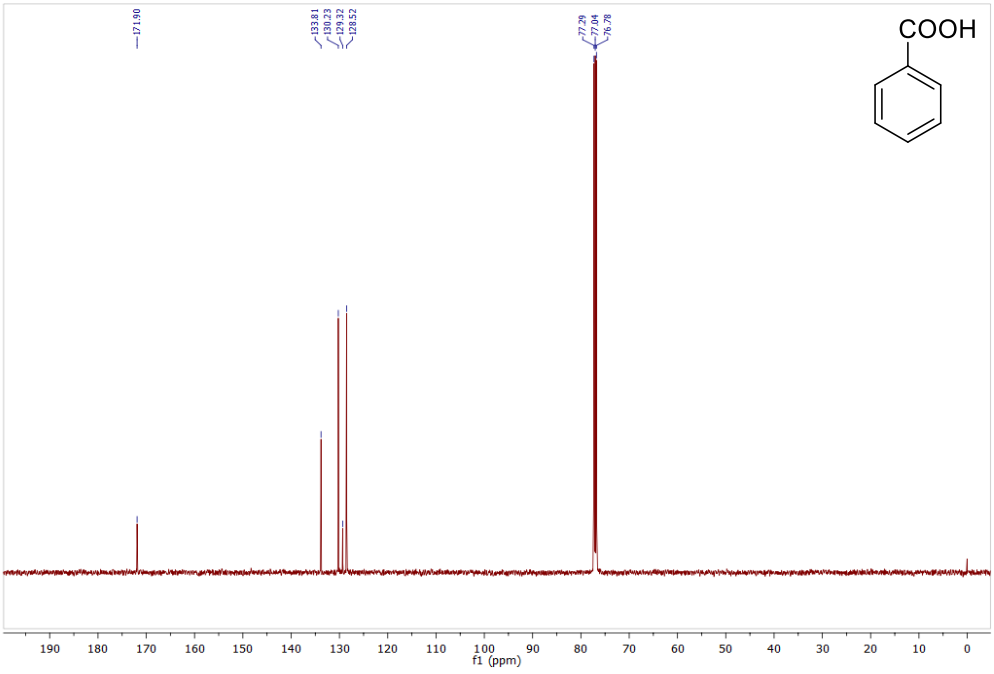

Figure S4. ^{13}C NMR spectrum of benzoic acid.

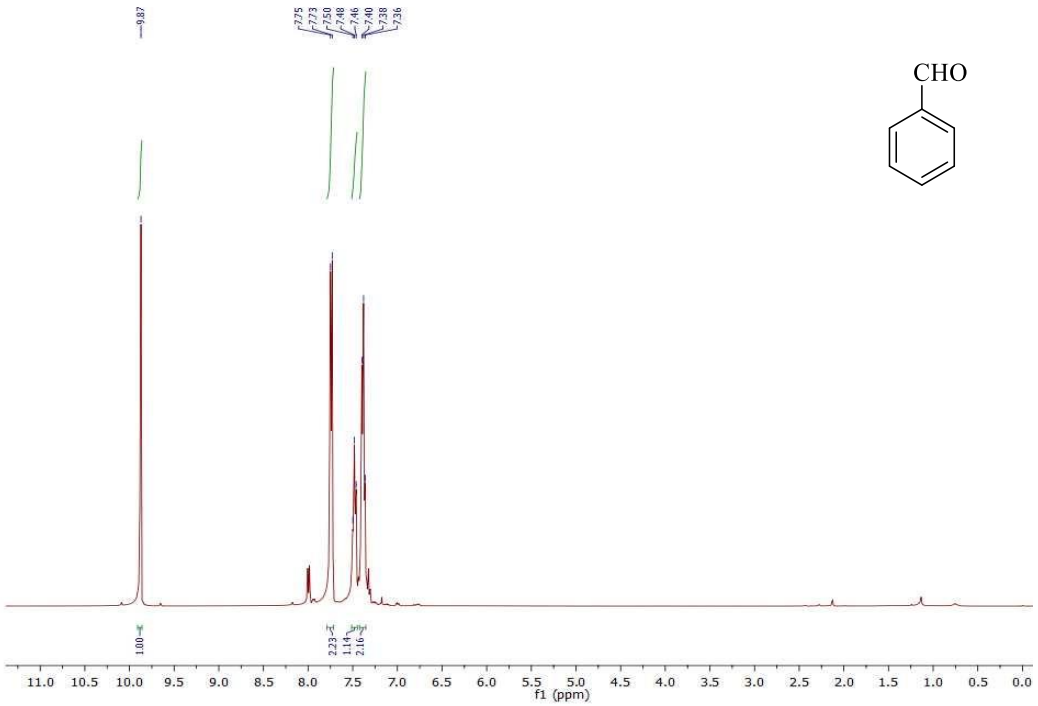

Figure S5. ^{1}H NMR spectrum of benzaldehyde.

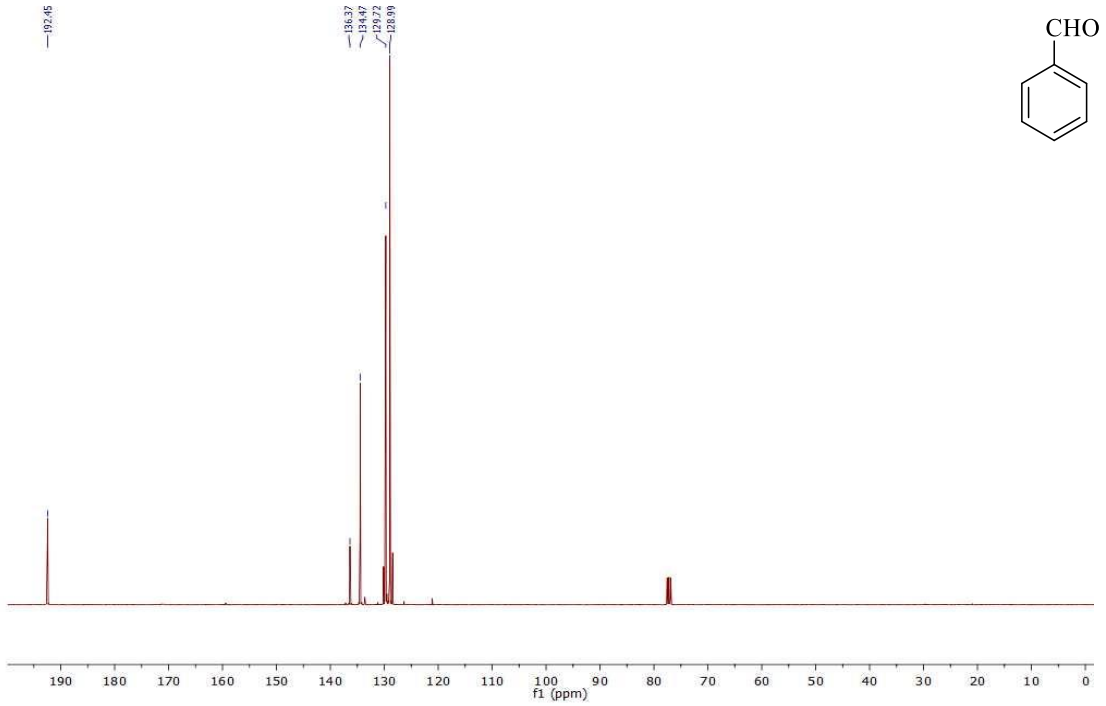

Figure S6. ^{13}C NMR spectrum of benzaldehyde.

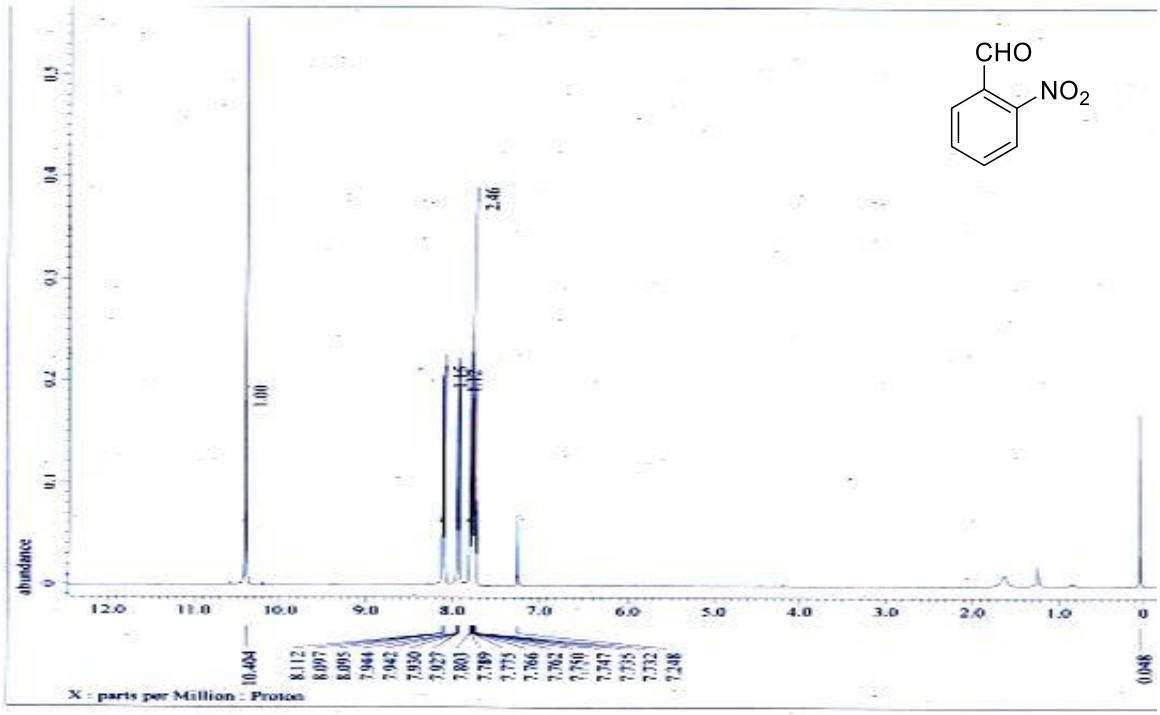

Figure S7. ^{1}H NMR spectrum of 2-nitrobenzaldehyde.

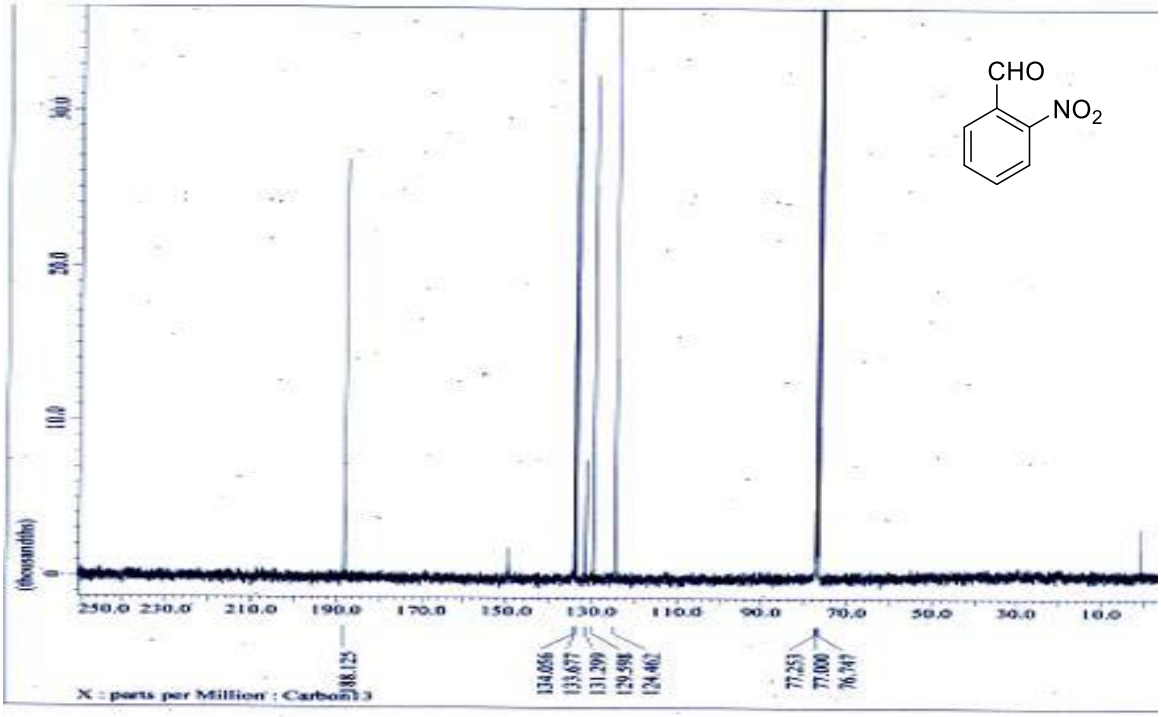

Figure S8. ^{13}C NMR spectrum of 2-nitrobenzaldehyde.

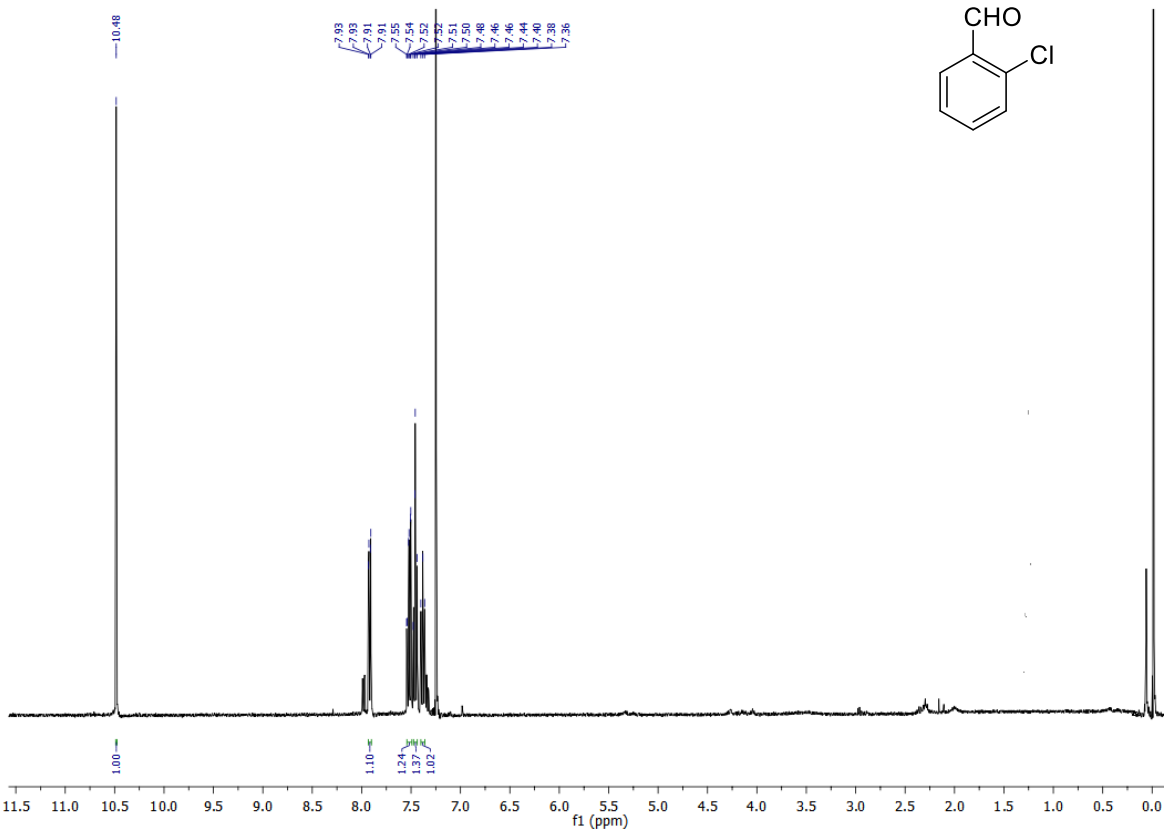

Figure S9. ^{1}H NMR spectrum of 2-chlorobenzaldehyde.

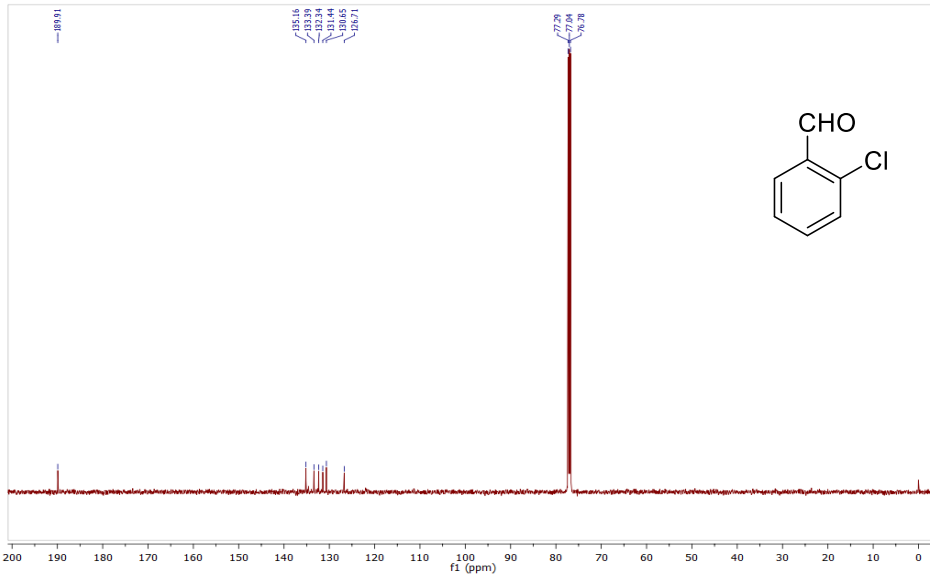

Figure S10. ^{13}C NMR spectrum of 2-chlorobenzaldehyde.

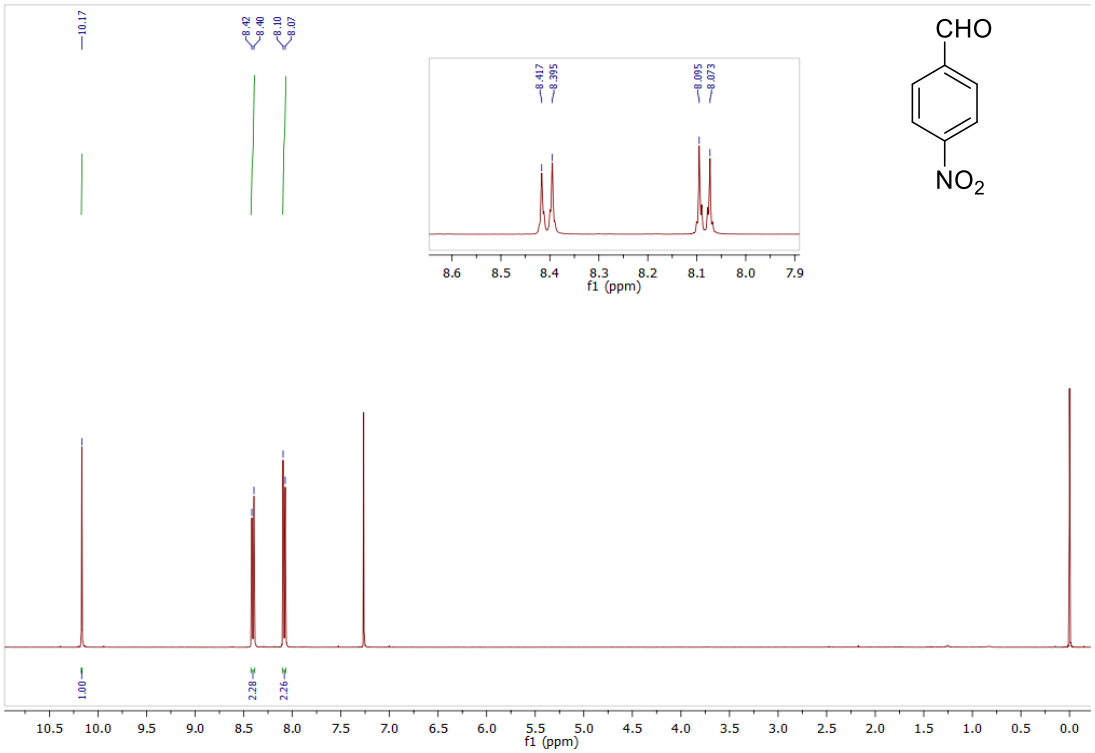

Figure S11. ^{1}H NMR spectrum of 4-nitrobenzaldehyde.

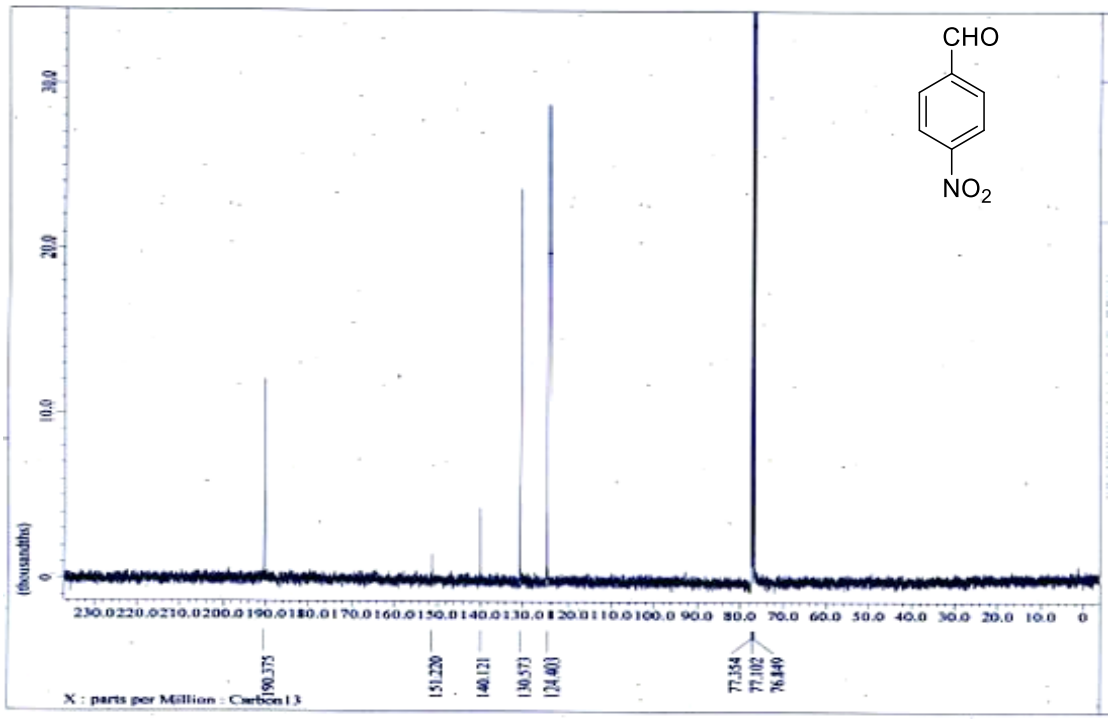

Figure S12. ^{13}C NMR spectrum of 4-nitrobenzaldehyde.

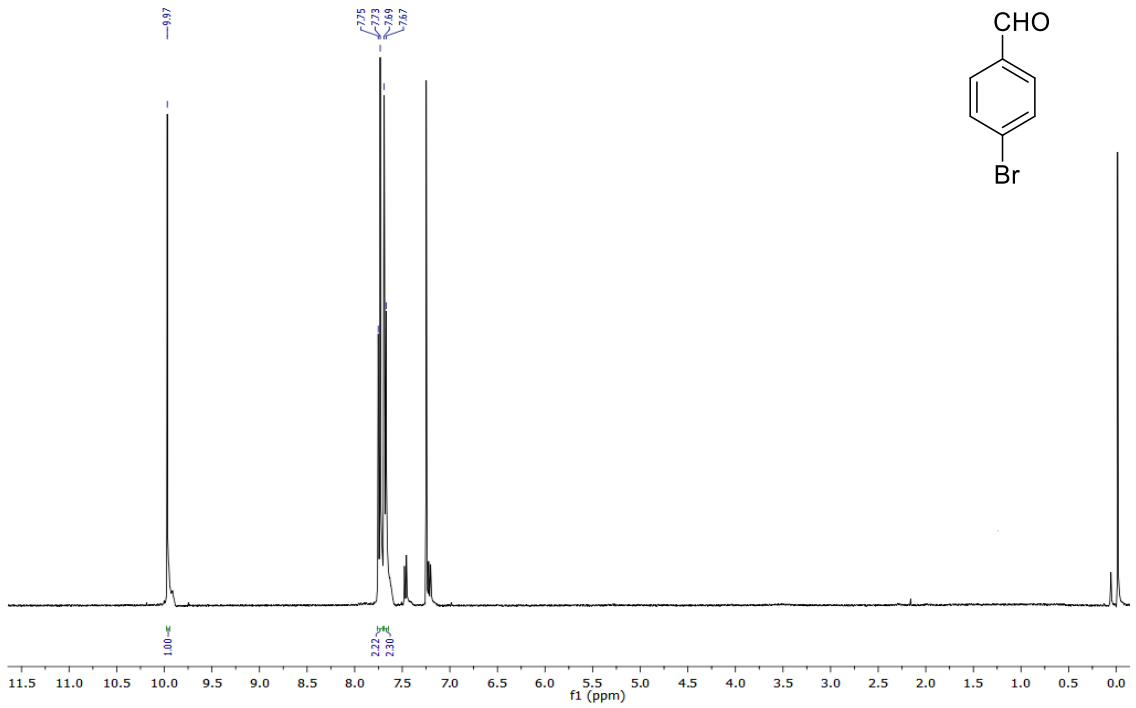

Figure S13. ^{1}H NMR of 4-bromobenzaldehyde.

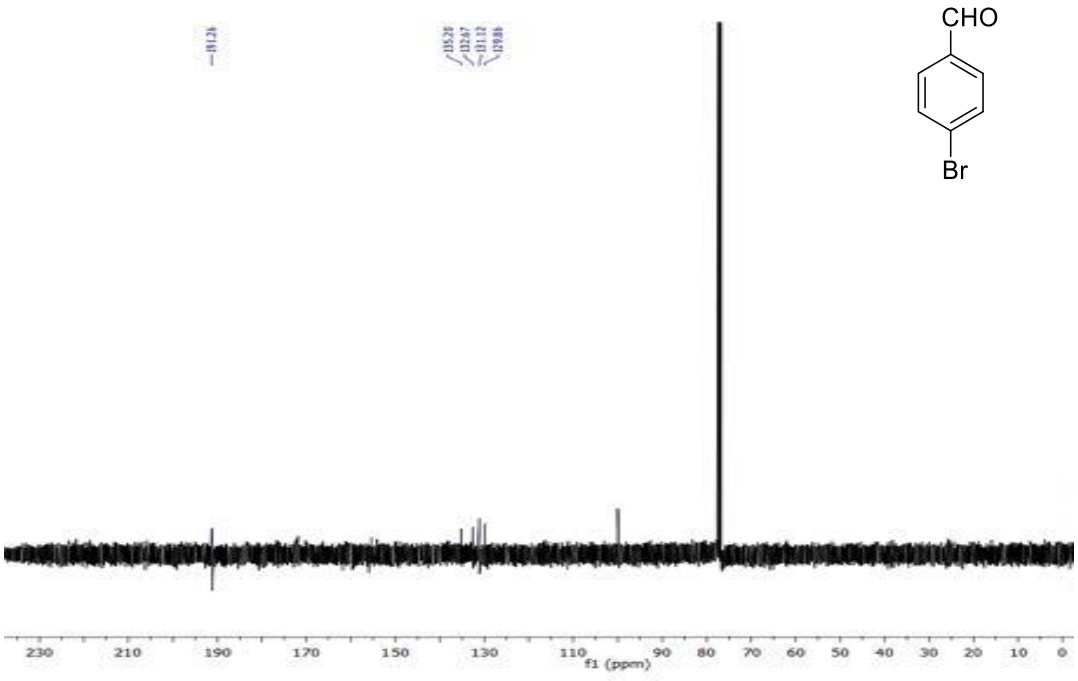

Figure S14. ^{13}C NMR of 4-bromobenzaldehyde.

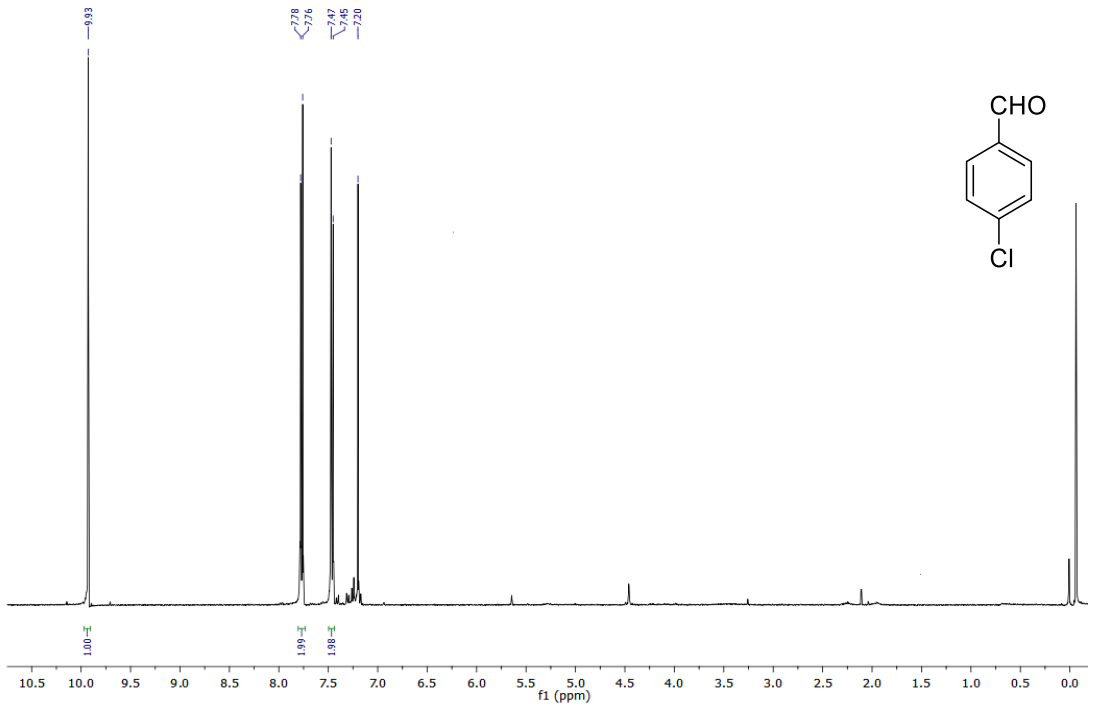

Figure S15. ^{1}H NMR of 4-chlorobenzaldehyde.

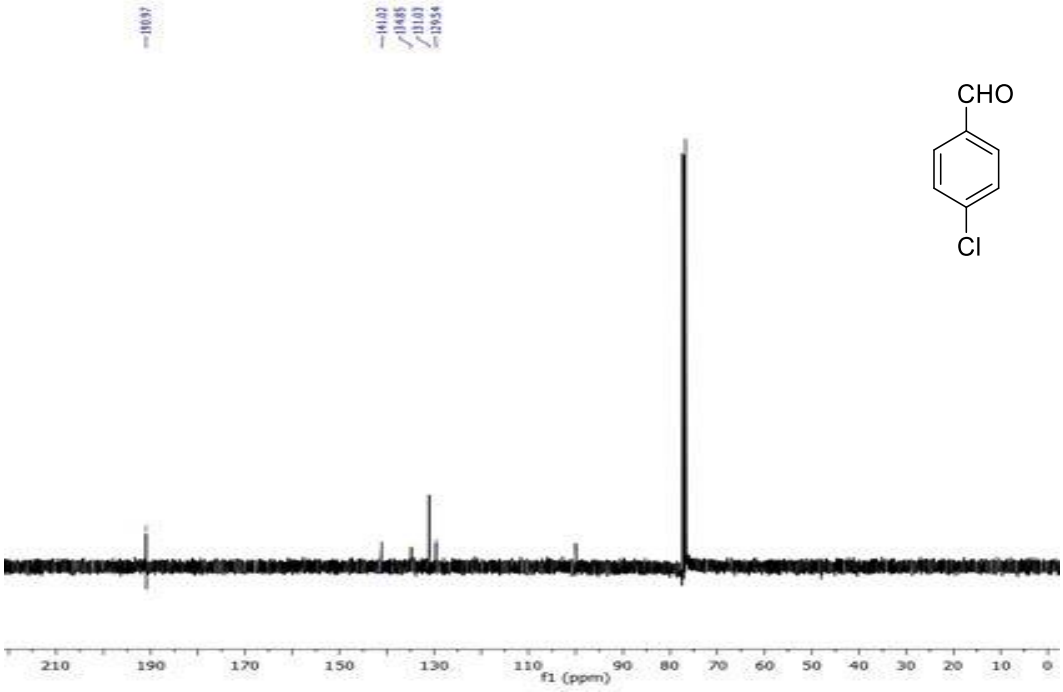

Figure S16. ^{13}C NMR of 4-chlorobenzaldehyde.

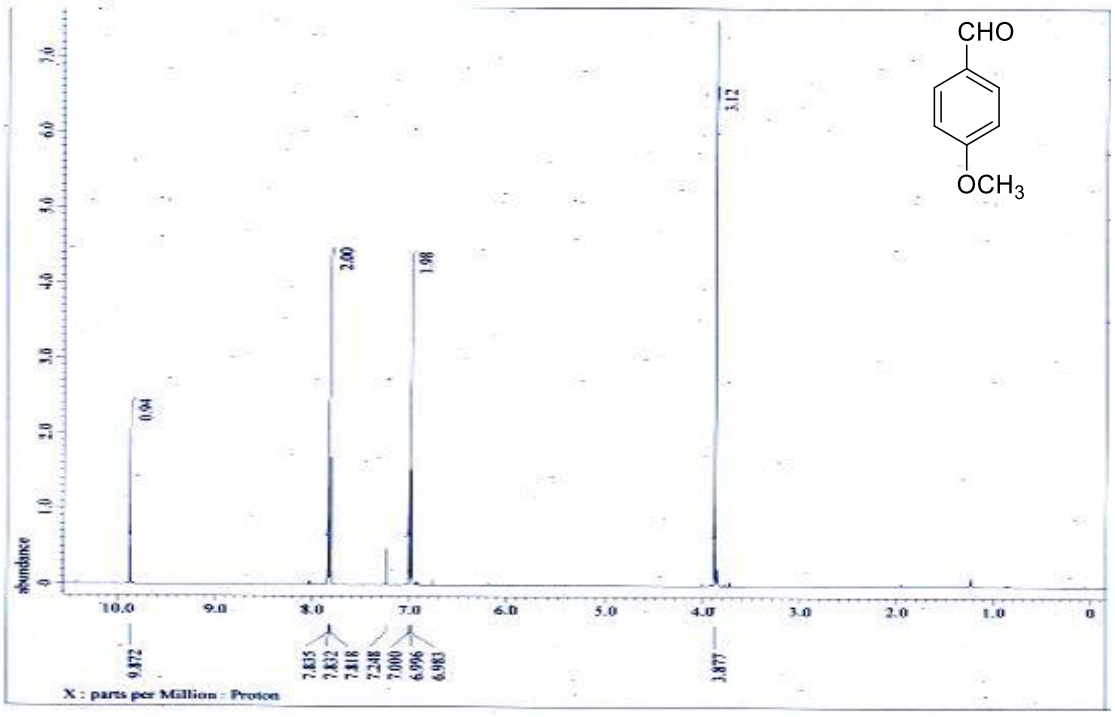

Figure S17. ^{1}H NMR spectrum of 4-methoxybenzaldehyde.

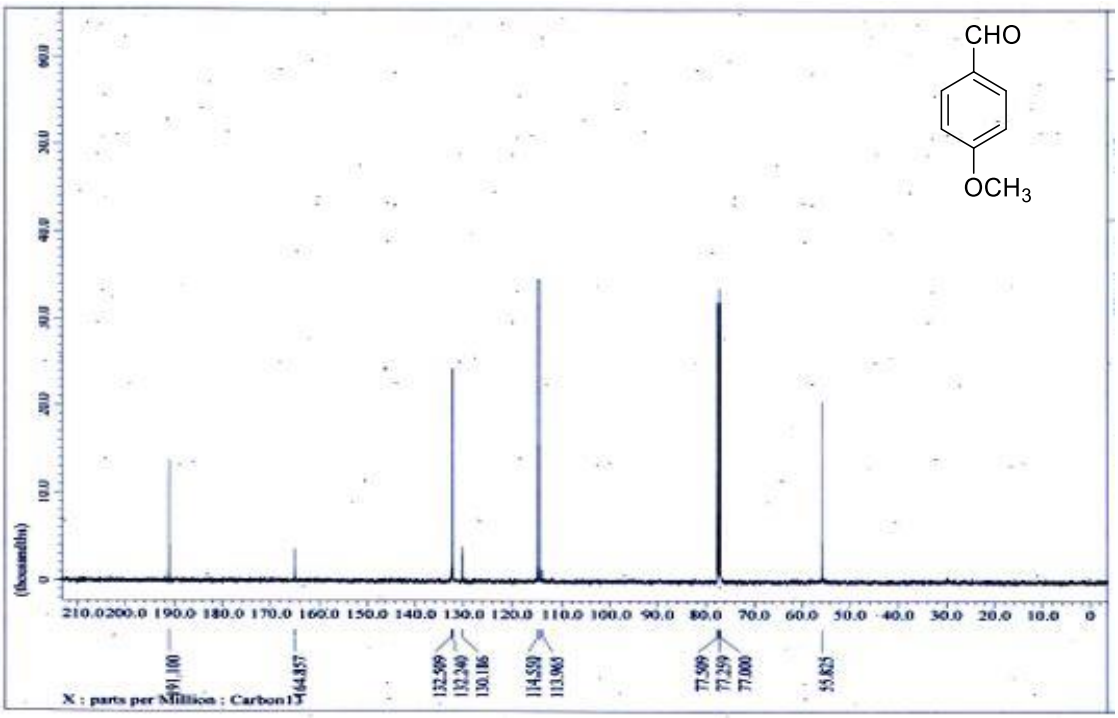

Figure S18. ^{13}C NMR spectrum of 4-methoxybenzaldehyde.

Reference.

1. Guan, X. et al. *New J. Chem.*, 2021, 45, 18192. https://doi.org/10.1039/D1NJ03145G